The 14-3-3 protein Bmh1 functions in the spindle position checkpoint by breaking Bfa1 asymmetry at yeast centrosomes

Ayse Koca Caydasi*, Yagmur Micoogullari*, Bahtiyar Kurtulmus, Saravanan Palani†, and Gislene Pereira
Molecular Biology of Centrosomes and Cilia, German Cancer Research Center, DKFZ-ZMBH Alliance, Heidelberg 69120, Germany

ABSTRACT **In addition to their well-known role in microtubule organization, centrosomes function as signaling platforms and regulate cell cycle events. An important example of such a function is the spindle position checkpoint (SPOC) of budding yeast. SPOC is a surveillance mechanism that ensures alignment of the mitotic spindle along the cell polarity axis. Upon spindle misalignment, phosphorylation of the SPOC component Bfa1 by Kin4 kinase engages the SPOC by changing the centrosome localization of Bfa1 from asymmetric (one centrosome) to symmetric (both centrosomes). Here we show that, unexpectedly, Kin4 alone is unable to break Bfa1 asymmetry at yeast centrosomes. Instead, phosphorylation of Bfa1 by Kin4 creates a docking site on Bfa1 for the 14-3-3 family protein Bmh1, which in turn weakens Bfa1–centrosome association and promotes symmetric Bfa1 localization. Consistently, *BMH1*-null cells are SPOC deficient. Our work thus identifies Bmh1 as a new SPOC component and refines the molecular mechanism that breaks Bfa1 centrosome asymmetry upon SPOC activation.**

Monitoring Editor
Rong Li
Stowers Institute

Received: Apr 14, 2014
Revised: May 6, 2014
Accepted: May 15, 2014

INTRODUCTION

The alignment of the mitotic spindle along the mother-to-daughter-cell polarity axis is critical for faithful chromosome segregation in budding yeast. A surveillance mechanism named the spindle position checkpoint (SPOC) ensures that cells do not exit mitosis and undergo cell division until the mitotic spindle is correctly positioned (Caydasi and Pereira, 2012). The SPOC prevents cells with misaligned spindles from exiting mitosis by inactivating the mitotic exit network (MEN; the signaling cascade that drives exit from mitosis; Bardin and Amon, 2001). The MEN is a centrosome-associated signaling cascade that drives exit from mitosis by controlling the localization of the phosphatase Cdc14. Active MEN releases Cdc14 from the nucleolus, allowing Cdc14 to dephosphorylate Cdk1 substrates and block Cdk1 activity by activating the Cdk1 inhibitor Sic1 and the anaphase-promoting complex (APC) subunit Cdh1 (Bardin and Amon, 2001). The SPOC inhibits the MEN by maintaining the activity of the bipartite GTPase-activating protein (GAP) complex composed of Bfa1 and Bub2 (Bardin *et al.*, 2000; Pereira *et al.*, 2000; Hu *et al.*, 2001). This in turn inactivates the GTPase Tem1, one of the most upstream MEN components (Geymonat *et al.*, 2002, 2003).

The Bfa1-Bub2 GAP complex localizes to the spindle pole bodies (SPBs; yeast equivalent of centrosomes) in a manner that depends on the relative positional context of the mitotic spindle. In an unperturbed mitosis, the levels of Bfa1-Bub2 GAP at the SPB that is directed toward the daughter cell (dSPB) are substantially higher than those found on the SPB that is retained in the mother cell body (Pereira *et al.*, 2000). In contrast, in cells with a misaligned spindle, Bfa1-Bub2 associates with equal intensity at both SPBs (symmetric localization; Pereira *et al.*, 2001; Caydasi and Pereira, 2009).

The SPB and mother cortex–associated kinase Kin4 participates in the mechanism that breaks the asymmetric SPB localization of Bfa1-Bub2 in response to spindle misalignment. Phosphorylation of

This article was published online ahead of print in MBoC in Press (http://www.molbiolcell.org/cgi/doi/10.1091/mbc.E14-04-0890) on May 21, 2014.

*These authors contributed equally to this work.

†Present address: Division of Biomedical Cell Biology, Warwick Medical School, University of Warwick, CV4 7AL Coventry, United Kingdom.

Address correspondence to: Gislene Pereira (g.pereira@dkfz.de).

Abbreviations used: APC, anaphase-promoting complex; dSPB, daughter-directed spindle pole body; GAP, GTPase-activating protein; MBP, maltose-binding protein; MEN, mitotic exit network; SAC, spindle assembly checkpoint; SPB, spindle pole body; SPOC, spindle position checkpoint.

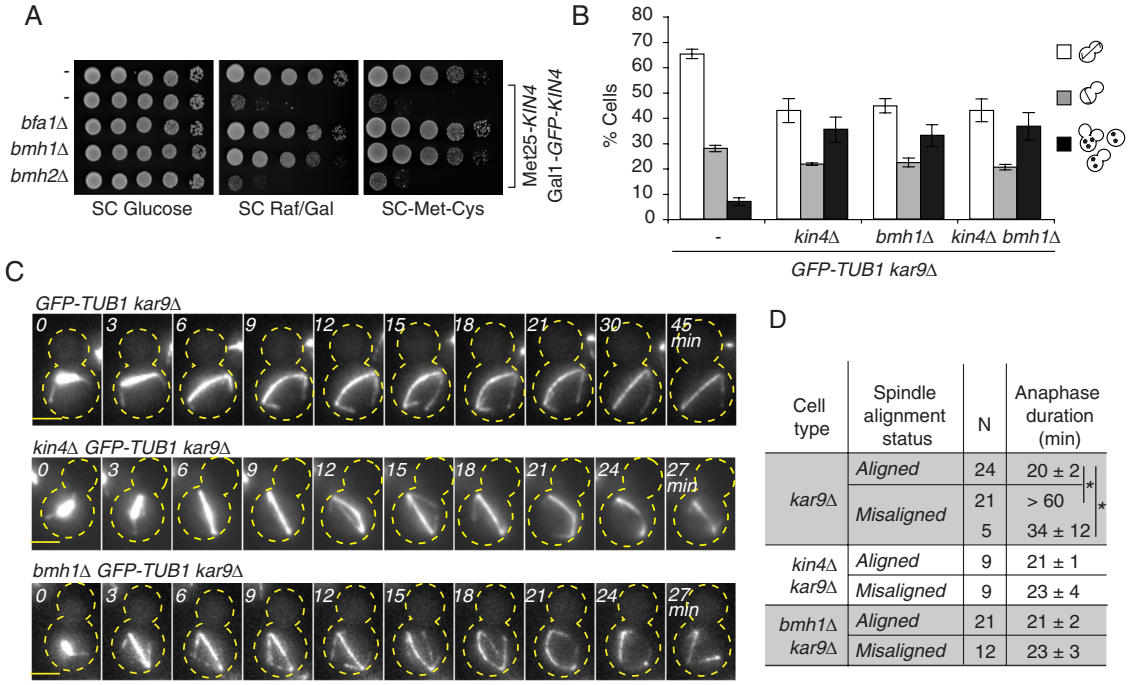

Cell type	Spindle alignment status	N	Anaphase duration (min)
kar9Δ	*Aligned*	24	20 ± 2 *
	Misaligned	21	> 60 *
		5	34 ± 12
kin4Δ kar9Δ	*Aligned*	9	21 ± 1
	Misaligned	9	23 ± 4
bmh1Δ kar9Δ	*Aligned*	21	21 ± 2
	Misaligned	12	23 ± 3

FIGURE 1: Bmh1 is a novel SPOC component. (A) Serial dilutions of the indicated strains were spotted on Gal1 and Met25–repressing (SC-glucose), Gal1-inducing (SC-Raf/Gal), and Met25-inducing (SC-Met-Cys) agar plates. (B) Percentage of cells with normal aligned (white bars) and misaligned (gray bars) anaphase spindles and with broken spindles in one cell body (black bars). Graph is the average of three independent experiments. Error bars, SEM. (C, D) Time-lapse analysis of *GFP-TUB1 kar9Δ* cells. (C) Representative still images for cells with misaligned spindles. Cell boundaries are marked by dashed lines. Scale bars, 3 μm. (D) Quantification of C, showing the anaphase duration during normal spindle alignment (aligned) and spindle misalignment (misaligned) in indicated cell types. Data represent mean ± SD. *N*, number of cells inspected. Asterisks indicate significant difference according to *t* test ($p < 0.05$).

Bfa1 by Kin4 decreases the residence time of the Bfa1-Bub2 complex at the dSPB and reduces the SPB bound Bfa1-Bub2 levels (Maekawa *et al.*, 2007; Caydasi and Pereira, 2009; Monje-Casas and Amon, 2009). The importance of this regulation is demonstrated by the fact that SPOC function is impaired when Bfa1 is forcibly retained at SPBs (Caydasi and Pereira, 2009). Removal of Bfa1 from SPBs might contribute to mitotic arrest via removal of a large pool of Tem1 from SPBs, where Tem1 activates the MEN (Valerio-Santiago and Monje-Casas, 2011; Caydasi *et al.*, 2012). In addition, redistribution of Bfa1-Bub2 from SPBs into the cytoplasm may also inhibit the small pool of Tem1 that is targeted to SPBs in a Bfa1-Bub2–independent manner (Caydasi *et al.*, 2012). However, how phosphorylation of Bfa1 by Kin4 alters the SPB-binding properties of Bfa1-Bub2 remains to be established.

Here we show that cells lacking *BMH1*, which belongs to the conserved 14-3-3 gene family (van Heusden and Steensma, 2006), fail to arrest in response to spindle misalignment. In vivo and in vitro assays revealed that Bmh1 specifically binds to Bfa1 molecules phosphorylated by Kin4. Using fluorescence microscopy–based techniques, we establish that Bmh1 and Kin4 act together to engage the SPOC by facilitating removal of Bfa1 from SPBs. Our study thus identifies and characterizes Bmh1 as a novel SPOC component.

RESULTS

Deletion of *BMH1* rescues the lethality of *KIN4* overexpression

KIN4 overexpression constitutively activates the Bfa1-Bub2 GAP complex, which in turn causes cell death through persistent inactivation of MEN signaling (D'Aquino *et al.*, 2005). In a genetic screen designed to uncover genes whose deletion rescued the toxicity of *KIN4* overexpression (Caydasi *et al.*, 2010), we identified *BMH1*. *bmh1Δ* cells were able to grow when *KIN4* was overexpressed from either the Gal1 or Met25 promoter (Figure 1A). Levels of overproduced Kin4 were comparable in *bmh1Δ* and *BMH1* cells (Supplemental Figure S1A). The growth rescue arose from deletion of *BMH1*, as it was reverted by a plasmid carrying wild-type *BMH1* (Supplemental Figure S1B).

BMH1 and its paralogue *BMH2* encode 14-3-3 family proteins in *Saccharomyces cerevisiae* (van Heusden and Steensma, 2006). Bmh1 and Bmh2 execute overlapping functions, depending on the context, as they can form heterodimers or homodimers that bind their ligands (Fu *et al.*, 2000; Shen *et al.*, 2003; Usui and Petrini, 2007; Wang *et al.*, 2009; Veisova *et al.*, 2010; Trembley *et al.*, 2014). *BMH1* but not *BMH2* was functionally linked to *KIN4* function because *BMH2* deletion failed to rescue lethality arising from *KIN4* overexpression (Figure 1A).

Bmh1 is essential for SPOC

We next asked whether *BMH1* participates in SPOC. In budding yeast, spindle orientation is under control of two redundant pathways, one dependent on the adenomatous polyposis coli–related protein Kar9 and the other on the microtubule motor protein dynein (Dyn1; McNally, 2013). Whereas simultaneous deletion of both *KAR9* and *DYN1* genes is lethal, individual deletion of *KAR9* or *DYN1* genes causes spindle misorientation at nonpermissive temperatures (Yeh *et al.*, 1995; Cottingham and Hoyt, 1997; Miller and Rose, 1998). In the absence of SPOC function, *kar9Δ* or *dyn1Δ* cells

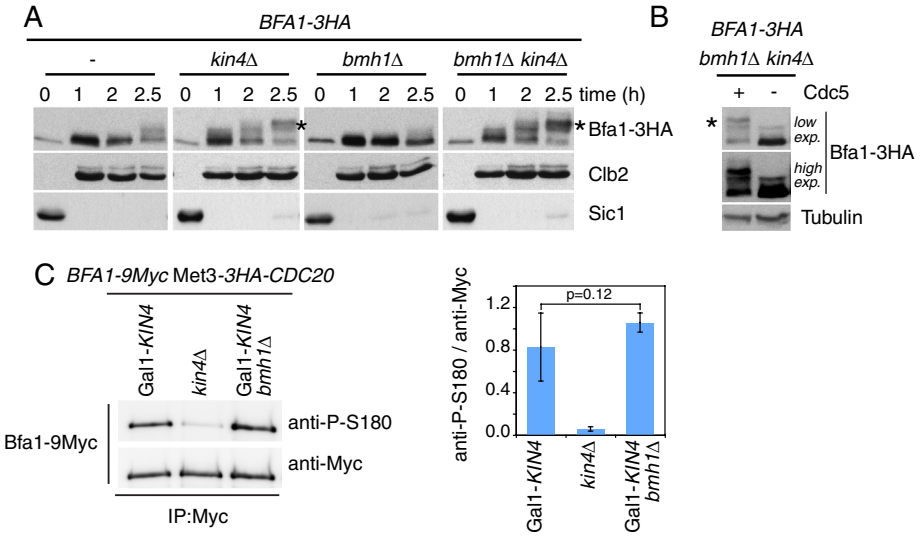

FIGURE 2: Bmh1 does not prevent Kin4 from phosphorylating Bfa1. (A, B) Immunoblots showing the phospho shift of Bfa1. (A) Cells were released from G1 block into nocodazole-containing medium. Clb2 and Sic1 served as markers for cell cycle progression. (B) *bmh1Δ kin4Δ* Gal1-*CDC5* cells were arrested in metaphase (nocodazole treatment) in *CDC5*-expressing (+Cdc5) or -repressing (–Cdc5) conditions. exp., exposure. Asterisks mark the Bfa1 hyperphosphorylated form. (C) Levels of Bfa1 phosphorylation at S180 residue by Kin4. Bfa1-9Myc was pulled down from yeast cell lysates arrested in metaphase by depletion of the APC subunit Cdc20, followed by addition of galactose to the medium to allow *KIN4* overexpression. Immunoblots were probed with the indicated antibodies. The graph shows the average of ratios obtained from six independent immunoblots of two independent experiments. Error bars, SD. The *p* value of the *t* test is indicated.

accumulate multiple nuclei or become anucleated because mitotic exit proceeds even when the anaphase spindle, hence the two DNA masses, resides in the mother cell body (Bardin *et al.*, 2000; Bloecher *et al.*, 2000; Pereira *et al.*, 2000). Using green fluorescent protein (GFP)–tagged tubulin (*GFP-TUB1*) as a microtubule marker, we monitored SPOC integrity in *kar9Δ bmh1Δ* cells (Figure 1B). We scored the percentage of cells with SPOC-deficient phenotypes alongside those with normal and misaligned anaphase spindles. Approximately 35% of *kar9Δ kin4Δ* cells were multinucleated, in contrast to only ~5% multinucleation in *kar9Δ* cells (Figure 1B, black bars). Remarkably, multinucleation frequency of *kar9Δ bmh1Δ* and *kar9Δ kin4Δ* cells was similar (Figure 1B). Simultaneous deletion of *BMH1* and *KIN4* in *kar9Δ* cells did not exacerbate the degree of SPOC deficiency observed in each individual deletion (Figure 1B), suggesting that Bmh1 and Kin4 exert mitotic arrest upon spindle misalignment by acting in the same pathway. Similar results were obtained with *dyn1Δ* cells (Supplemental Figure S2A). Thus Bmh1 is required to engage the SPOC regardless of the spindle orientation pathway that was perturbed.

Next we performed live-cell imaging of *kar9Δ GFP-TUB1* cells (Figure 1C) and calculated the duration of anaphase as the time elapsed between the onset of fast spindle elongation and spindle breakdown. In all cell types, anaphase took ~20 min when the spindle was correctly aligned (Figure 1D). The vast majority of *kar9Δ* cells with a misaligned spindle were arrested in anaphase with an intact spindle ($t > 60$ min; Figure 1D). In contrast, *bmh1Δ kar9Δ* and *kin4Δ kar9Δ* cells disassembled the misaligned spindle with similar timing as cells with correctly aligned spindles (Figure 1D). Therefore Bmh1 is crucial to halt mitotic exit in response to spindle misorientation.

The SPOC components Bfa1 and Bub2, but not Kin4, are indispensable for the cell cycle arrest in response to microtubule depolymerization that activates the spindle assembly checkpoint (SAC; Hoyt *et al.*, 1991; Li and Murray, 1991; Fraschini *et al.*, 1999; D'Aquino *et al.*, 2005; Pereira and Schiebel, 2005). The SAC inhibits the degradation of securin/Pds1 upon microtubule depolymerization to restrain the separation of sister chromatids until all kinetochores have attached to the microtubules in a bipolar manner (Foley and Kapoor, 2013). We therefore asked whether Bmh1 is required for SAC activity. To this end, we analyzed the ability of *bmh1Δ* cells to arrest mitotic progression upon microtubule depolymerization by nocodazole treatment. Wild-type cells arrested as large-budded cells with high levels of securin/Pds1 and mitotic cyclin Clb2, whereas SAC-deficient *bub2Δ* and *mad2Δ* cells degraded securin/Pds1 and Clb2 (Supplemental Figure S2B) and reassumed the cell cycle (multiple-budded cells, Supplemental Figure S2C). *bmh1Δ* cells resembled wild-type cells, as they arrested in metaphase with high securin/Pds1 and Clb2 levels (Supplemental Figure S2, B and C). Therefore we concluded that Bmh1, like Kin4, plays a role in SPOC but not SAC.

Bmh1 does not influence Kin4 kinase activity and localization

To understand the mechanism by which Bmh1 functions in SPOC, we analyzed whether Bmh1 acts upon Kin4. In the absence of Bmh1, Kin4 cellular localization and in vitro ability to phosphorylate Bfa1 were similar to those for wild-type cells (Supplemental Figure S3, A–C). To evaluate Kin4 activity in vivo, we assessed the phosphorylation profile of Bfa1 by monitoring Bfa1 mobility shift on protein gels. It is well established that Kin4 phosphorylates Bfa1 to prevent the inhibitory phosphorylation of Bfa1 by the polo-like kinase Cdc5 (Maekawa *et al.*, 2007). Cdc5-dependent phosphorylation of Bfa1 generates forms of Bfa1 that migrate more slowly in SDS–PAGE. These slow-migrating forms become apparent in nocodazole-treated cells only when Kin4 phosphorylation of Bfa1 is abolished (Hu *et al.*, 2001; Pereira and Schiebel, 2005; Maekawa *et al.*, 2007). Accordingly, slow-migrating forms of Bfa1-3HA appeared in metaphase-arrested *kin4Δ* cells (Figure 2A, asterisk). These slow-migrating forms of Bfa1 were absent in *bmh1Δ* cells (Figure 2A). Of importance, deletion of *KIN4* in the *bmh1Δ* strain background promoted the phospho shift of Bfa1 (Figure 2A, asterisk), which was abolished upon depletion of Cdc5 (Figure 2B). This implies that phosphoregulation of Bfa1 by Kin4 and Cdc5 is not affected by deletion of *BMH1*.

To evaluate Kin4 activity in vivo, we monitored the phosphorylation of Bfa1 by Kin4 with a phospho-specific antibody that had been raised to recognize Bfa1 when phosphorylated on S180 (P-S180; one of the two serines phosphorylated by Kin4; Maekawa *et al.*, 2007). Anti–P-S180 antibodies recognized Bfa1 when Bfa1 was immunoprecipitated from yeast cells overexpressing *KIN4* but not when it was immunoprecipitated from *kin4Δ* cells (Maekawa *et al.*, 2007; Figure 2C and Supplemental Figure S3D). The level of P-S180 did not decline in *bmh1Δ* cells (Figure 2C). Thus Bmh1 is not required for overproduced Kin4 to phosphorylate Bfa1. Collectively these data indicate that Bmh1 does not influence Kin4 localization or catalytic activity toward Bfa1 in vitro and in vivo.

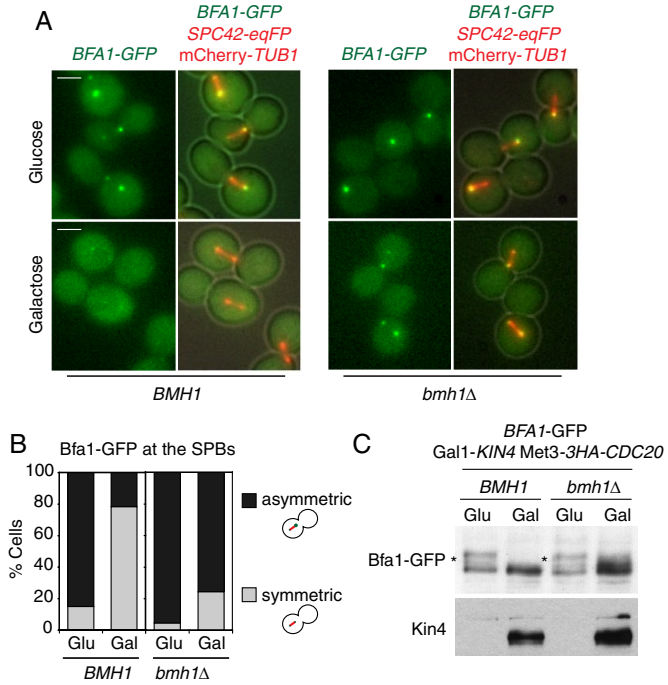

FIGURE 3: Bmh1 is required for Kin4-induced change in Bfa1 localization. (A–C) Gal1-*KIN4* was repressed (glucose [Glu]) or induced (galactose [Gal]) in Met3-*3HA-CDC20* Gal1-*KIN4* cells arrested in metaphase by Cdc20 depletion. Localization of Bfa1-GFP at SPBs was compared in wild-type and *bmh1Δ* cells with or without *KIN4* overexpression. (A) Representative still images and (B) quantification of cells with symmetric and asymmetric Bfa1-GFP at the SPBs. More than 100 cells were counted per sample. (C) Kin4 protein levels were detected by immunoblots using anti-Kin4 antibody. Note that the shift in Bfa1 protein band under Kin4 depleted conditions (marked by asterisk) disappears upon *KIN4* overexpression in both *BMH1* and *bmh1Δ* cells.

Bmh1 regulates SPB localization of Bfa1

Phosphorylation of Bfa1 by Kin4 disrupts the asymmetric SPB localization of the Bfa1-Bub2 complex, a process that is required to engage the SPOC (Caydasi and Pereira, 2009; Monje-Casas and Amon, 2009). To examine whether Bmh1 controls Bfa1 localization, we first determined Bfa1 SPB localization in *bmh1Δ* cells upon *KIN4* overexpression. Because *bmh1Δ* cells do not arrest in anaphase when *KIN4* is overexpressed, we arrested both wild-type and *bmh1Δ* cells in metaphase by depleting the APC subunit Cdc20 before inducing *KIN4* overexpression. As reported (Caydasi and Pereira, 2009), Bfa1 preferentially and strongly associated with the dSPB in metaphase-arrested cells (Figure 3A, glucose) but bound equally at diminished levels to both SPBs in response to Kin4 overproduction (Figure 3A, galactose). This dramatic change in Bfa1 localization induced by Kin4 was not observed in *bmh1Δ* cells (Figure 3, A and B) despite elevated Kin4 levels (Figure 3C). Moreover, the Bfa1 pattern on protein gels that reflects Bfa1 phosphorylation was equal between wild-type and *bmh1Δ* cells (Figure 3C). This suggests that Kin4 phosphorylation of Bfa1 is not sufficient to change Bfa1-SPB localization in the absence of *BMH1*. Remarkably, metaphase-arrested *bmh1Δ* cells under Kin4-repressing conditions had a tendency for stronger Bfa1 asymmetry at the SPBs (i.e., complete loss of Bfa1 localization from one SPB) than *BMH1* cells (Figure 3 and Supplemental Figure S4). Elevated levels of Kin4 were able to reduce this tendency to some extent, implying that overproduced Kin4 might slightly affect Bfa1 localization in a Bmh1-independent manner.

We next analyzed the importance of Bmh1 for Bfa1 localization in case of spindle misalignment. Bfa1 localized symmetrically (with equal intensity at both SPBs) in the majority of *kar9Δ* cells with misaligned spindles (Figure 4A). In contrast, Bfa1 localization was largely asymmetric in *bmh1Δ kar9Δ* cells (Figure 4A). Analysis of Bub2 localization during spindle misalignment gave similar results (Supplemental Figure S5). This behavior was reminiscent of the previously reported *kin4Δ kar9Δ* phenotype (Caydasi and Pereira, 2009). Monitoring Bfa1-GFP by time-lapse microscopy in *kar9Δ* cells confirmed that Bfa1 became symmetric during the anaphase spindle elongation that occurred within the mother cell body of wild-type cells, whereas it remained asymmetric when *BMH1* had been deleted (Figure 4, B and C). Collectively these data indicate that Bmh1 is involved in the control of Bfa1 SPB localization in response to spindle misalignment.

Bmh1 binds only to Kin4-phosphorylated Bfa1

Given that 14-3-3 binds to phosphorylated proteins (Fu *et al.*, 2000), we asked whether Bmh1 specifically recognizes Bfa1 molecules that were phosphorylated by Kin4. We tested this hypothesis in vitro using yeast-enriched glutathione *S*-transferase (GST)–Kin4 and recombinant Bfa1 and Bmh1 proteins (Figure 5A). GST-Bmh1 failed to bind nonphosphorylated maltose-binding protein (MBP)–Bfa1 (Bfa1 fused to MBP; Figure 5B, lane 9), but it efficiently associated with MBP-Bfa1 that was prephosphorylated with Kin4 (Figure 5B, lane 1). The preincubation of MBP-Bfa1 with inactive Kin4 (GST-Kin4^{T209A}) did not promote the binding of Bfa1 to Bmh1 (Figure 5B, lane 5). Furthermore, a nonphosphorylatable Bfa1 mutant protein (MBP-Bfa1^{2A}) in which the two serine residues (S150 and S180) that are phosphorylated by Kin4 (Maekawa *et al.*, 2007) were mutated to alanine did not interact with GST-Bmh1 after Kin4 pre-phosphorylation (Figure 5B, lane 4). Of interest, the single nonphosphorylatable Bfa1^{S150A} and Bfa1^{S180A} mutants also failed to bind Bmh1, although they were phosphorylated at the nonmutated serine residue by Kin4 (Figure 5B, lanes 2 and 3). Thus the association between Bmh1 and Bfa1 requires Kin4 phosphorylation of both S150 and S180 residues on Bfa1.

We next asked whether Bfa1 and Bmh1 interact in vivo. Bfa1-3HA coimmunoprecipitated with Bmh1-3Myc (Figure 6A, lane 3), indicating that they are part of the same complex. Kin4 was required for association of Bfa1 with Bmh1, as the level of Bfa1 that coimmunoprecipitated with Bmh1 was drastically reduced in *kin4Δ* cells (Figure 6A, lanes 3 and 4). The binding of Bfa1^{2A} to Bmh1 was also greatly reduced, although not as severely as seen in *kin4Δ* cells (Figure 6B, lanes 3 and 4). Together our data show that phosphorylation of Bfa1 at S150 and S180 by Kin4 creates a docking site for Bmh1.

Bmh1 disturbs the stable association of Bfa1 with SPBs

In a normal anaphase, Bfa1 stably associates with the dSPB. Through phosphorylation of Bfa1 by Kin4, this Bfa1 pool becomes mobilized (Caydasi and Pereira, 2009; Monje-Casas and Amon, 2009). We therefore investigated the possibility that Bmh1 mobilizes Bfa1 at SPBs. We reasoned that if this was the case, Bfa1 would remain stably associated with SPBs in *bmh1Δ* cells with misaligned spindles. To test this hypothesis, we performed fluorescence recovery after photobleaching (FRAP) experiments. In wild-type cells, SPB-associated Bfa1-GFP became dynamic during spindle misalignment (Figure 7A; $t_{1/2} = 19 \pm 8$ s; mobile fraction, 100%). In sharp contrast, 50% of SPB-bound Bfa1 was stably associated with the SPB in

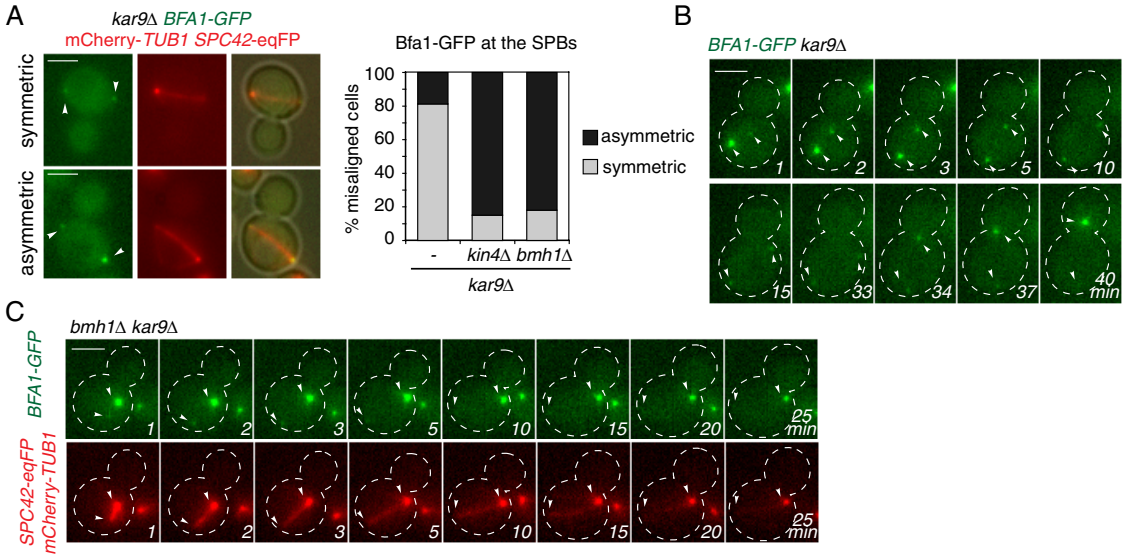

FIGURE 4: Bmh1 controls Bfa1 SPB localization upon spindle misalignment. (A) Representative images and percentage of misaligned spindles with symmetric and asymmetric Bfa1-GFP localization at SPBs of *kar9Δ* cells. Spc42-eqFP and mCherry-*TUB1* served as SPB and spindle markers, respectively. Note that Spc42-eqFP appears weaker in the new SPB due to slow maturation properties of the fluorophore (Pereira *et al.*, 2001). More than 50 misaligned spindles were counted from each strain. (B, C) Representative still images of a time-lapse series showing Bfa1-GFP localization at SPBs during spindle misalignment in cells with (B) or without (C) *BMH1*. Note that in B, Bfa1 levels decreased at SPBs during spindle elongation in the mother cell body (spindle misaligned: 1–33 min) and increased at daughter-directed SPB after spindle realignment (34–40 min). Arrows mark SPBs. Dashed line indicates the cell boundaries. Scale bars, 3 μm.

bmh1Δ cells with a misaligned spindle, as was the case for *kin4Δ* cells (Figure 7, B and C). In addition, the half-life of recovery for the mobile fraction of Bfa1 in *bmh1Δ* cells ($t_{1/2}$ = 40 ± 16 s) was twofold slower than in wild-type cells ($t_{1/2}$ = 19 ± 8 s) and slightly faster than in *kin4Δ* cells ($t_{1/2}$ = 68 ± 29 s). These data indicate that the change in Bfa1-SPB binding dynamics upon SPOC activation requires the functions of both Bmh1 and Kin4.

DISCUSSION

Here we established that removal of *BMH1* suppressed the growth toxicity arising from *KIN4* overexpression. Deletion of *BMH1* has been reported to confer growth sensitivity to benomyl, a microtubule-depolymerizing drug that requires both SAC and the SPOC components Bfa1 and Bub2 for survival (Grandin and Charbonneau, 2008). Our data show that Bmh1 is specifically required to engage the SPOC but not the SAC. We further established that, among the yeast 14-3-3 family proteins, SPOC function is governed by Bmh1, as deletion of *BMH2* neither rescued Kin4 overexpression toxicity nor exhibited significant SPOC deficiency (unpublished data).

Our data are consistent with the following model. In the SPOC-arrested state, Kin4 phosphorylates Bfa1, but this event per se is unable to promote the displacement of Bfa1 from SPBs to provide a robust SPOC arrest. Instead, Kin4 phosphorylation creates a docking site for Bmh1, which, in turn, promotes a decline in Bfa1 residence time and protein levels at SPBs (Figure 8). Several lines of evidence support this model. First, deletion of *BMH1* led to a similar deficiency in SPOC function as *KIN4* deletion; however it had no effect on Kin4's ability to phosphorylate Bfa1 in vivo and in vitro. Second, in vivo and in vitro binding experiments established that Bmh1 binds Bfa1 specifically when Bfa1 is phosphorylated by Kin4 at both serines 150 and 180. These residues fulfill the common properties of Bmh1-binding motifs that generally overlap with the sites phosphorylated by the AMP-activated protein kinase family of kinases to which Kin4 belongs (Johnson *et al.*, 2010). Third, the switch from asymmetric to symmetric Bfa1 SPB localization and the change in SPB binding dynamics during spindle misalignment or upon elevation of Kin4 levels required both Bmh1 and the phosphorylation of Bfa1 by Kin4. This regulation of Bfa1 localization seems to be restricted to the SPOC-activated state, as Bfa1 localization during an unperturbed anaphase was not altered upon deletion of *BMH1* or *KIN4* (unpublished data; Caydasi and Pereira, 2009).

14-3-3 affects the function of its binding partners in different ways, including stimulation or inhibition of protein–protein interactions, regulation of activity, and alteration of protein localization (van Heusden and Steensma, 2006). It is thus likely that the binding of Bmh1 to Kin4 phosphorylated Bfa1 weakens Bfa1-SPB binding or removes it completely from a particular receptor at the SPBs, which in turn might cause the decrease of Bfa1 levels and residence time at the SPBs.

It has been reported that 14-3-3 targets contain one, two, or more phosphorylated 14-3-3–binding sites (Yaffe, 2002; Johnson *et al.*, 2010). We found that phosphorylation of two (S150 and S180) residues in Bfa1 was required for the binding of Bmh1 to Bfa1 in vitro and in vivo. The two 14-3-3–binding sites on Bfa1 might bind to either side of a Bmh1 dimer, as shown for some 14-3-3 targets with two phosphorylated 14-3-3–binding motifs (Kostelecky *et al.*, 2009). It has been demonstrated that two phosphorylated 14-3-3–binding motifs on the same target protein enhance 14-3-3 binding compared with single-phosphorylated motifs (Yaffe *et al.*, 1997; Kostelecky *et al.*, 2009). Similarly, the presence of a dual 14-3-3–binding motif in Bfa1 might be required to create high-affinity Bmh1-binding sites. The two Bmh1-binding sites of Bfa1 are separated from each other with a short stretch of 30 amino acid residues. Of interest, the binding of 14-3-3 to targets with paired phosphorylated sites separated by <40 amino acids was proposed to

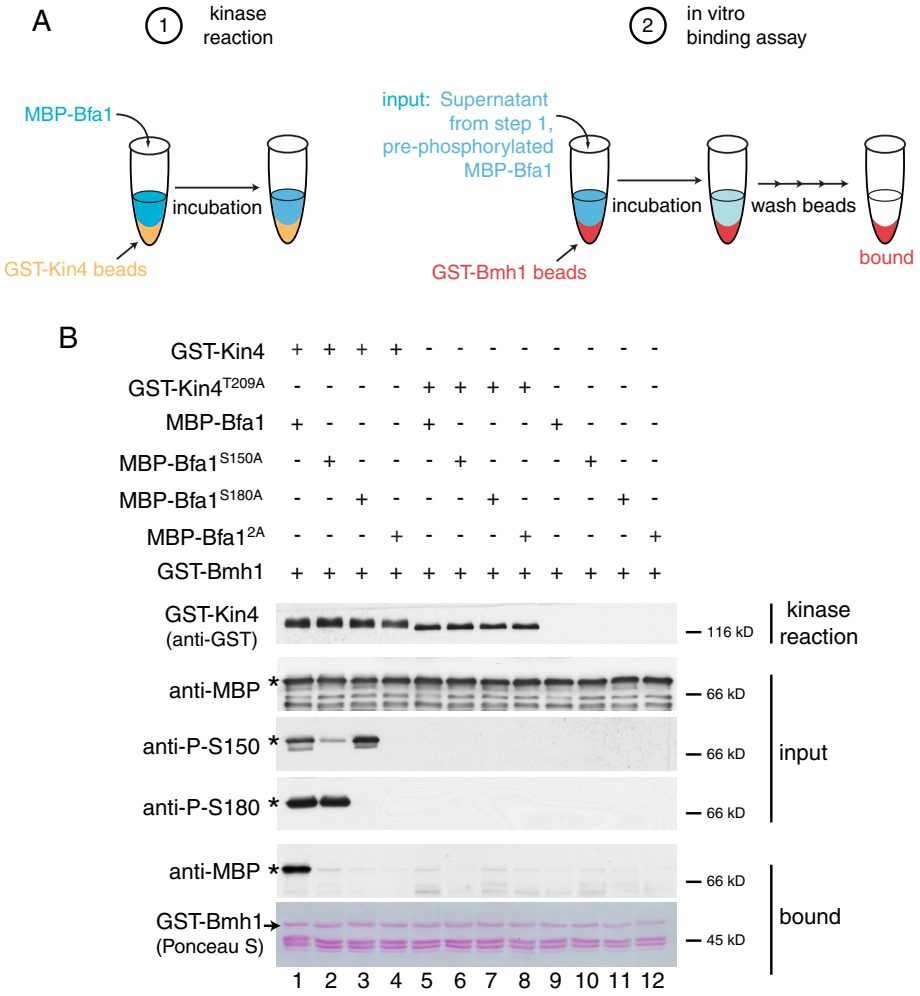

FIGURE 5: Bmh1 binds to Kin4 phosphorylated Bfa1 in vitro. (A, B) In vitro binding assay using yeast-enriched GST-Kin4 and recombinant-purified MBP-Bfa1 and GST-Bmh1. (A) Schematic representation of the experimental setup. (B) MBP-Bfa1 (lanes 1, 5, and 9), MBP-Bfa1^{S150A} (lanes 2, 6, and 10), MBP-Bfa1^{S180A} (lanes 3, 7, and 11), or MBP-Bfa1^{2A} (lanes 4, 8, and 12) were incubated with catalytic active Kin4 (GST-Kin4, lanes 1–4), kinase-dead Kin4 (GST-Kin4^{T209A}, lanes 5–8), or buffer only (lanes 9–12). MBP-Bfa1 bound to GST-Bmh1 beads was detected using anti-MBP antibodies. Phosphorylation of MBP-Bfa1 by Kin4 was confirmed using anti–P-S150 and anti–P-S180 antibodies. Asterisks show a degradation product of MBP-Bfa1 that is effectively phosphorylated by Kin4 in vitro (Maekawa *et al.*, 2007). The arrow indicates full-length GST-Bmh1 after Ponceau S staining.

affect the conformation of the target (Obsilova *et al.*, 2008; Johnson *et al.*, 2010). It is thus tempting to speculate that Bmh1 might cause structural changes in Bfa1, thereby altering the SPB-binding properties of Bfa1-Bub2 GAP complex.

Where do Bfa1 and Bmh1 interact? We were not able to detect Bmh1 at SPBs mainly because Bmh1 is a very abundant protein that strongly resides in the nucleus and cytoplasm (unpublished data). Therefore we suggest that a small transient pool of Bmh1 might associate with Bfa1 at SPBs to facilitate its release in the cytoplasm. Bmh1 and Bfa1 might also form a stable complex in the cytoplasm, which might in turn prevent Bfa1 recruitment to SPBs.

The SPOC component Kin4 both prevents Cdc5 phosphorylation of Bfa1 and disturbs the stable association of Bfa1 with SPBs (Maekawa *et al.*, 2007; Caydasi and Pereira, 2009). How these two events are mechanistically interlinked is not fully understood. The dissociation of Bfa1 from the SPBs could help prevent its phosphorylation by Cdc5, by moving the Cdc5 substrate Bfa1 from this kinase at SPBs, as we previously suggested (Caydasi and Pereira, 2009). However, our data now indicate that Kin4 may have an additional function in inhibiting the phosphorylation of Bfa1 by Cdc5 at SPBs. In the absence of Bmh1, Bfa1 remains stably associated with SPBs during spindle misalignment, yet Bfa1 was phosphorylated by Kin4. However, no hyperphosphorylation of Bfa1 by Cdc5 was observed in *bmh1Δ* cells, in contrast to *bmh1Δ kin4Δ* cells. Therefore it is unlikely that Kin4-modified Bfa1 is protected from Cdc5 phosphorylation solely through the promotion of the dissociation of Bfa1 from SPBs. Because Cdc5 is able to phosphorylate Kin4-phosphorylated Bfa1 in vitro (Maekawa *et al.*, 2007), it is also unlikely that Kin4 phosphorylated Bfa1 is not recognized by Cdc5. We therefore propose that the mechanism by which Bfa1 escapes from the action of Cdc5 at SPBs requires Kin4 and may involve further factors other than Bmh1 that remain to be identified.

The 14-3-3 family proteins participate in diverse physiological responses that also impinge upon cell cycle progression, such as TOR-mediated growth control, stress response, cytokinesis, and DNA-damage checkpoint (Gardino and Yaffe, 2011). Our data now expand this list of 14-3-3 functions, revealing a role in the regulation of protein localization at yeast centrosomes. This control is required to coordinate timely execution of mitotic exit with the correct position of the mitotic spindle. 14-3-3 associates with mammalian centrosomes, and several interaction partners of 14-3-3 are also centrosome-associated proteins (Pietromonaco *et al.*, 1996; Bolton *et al.*, 2008; Molla-Herman *et al.*, 2008). Given that the functional link between 14-3-3 binding and centrosome localization of 14-3-3–interacting proteins has not been studied in depth, it would be interesting to investigate whether 14-3-3 members of higher eukaryotes contribute to cell cycle regulation and/or centrosome-related functions by controlling protein binding dynamics at centrosomes.

MATERIALS AND METHODS

Yeast strains, plasmids, and growth conditions

Yeast strains and plasmids used in this study are listed in Supplemental Table S1. All yeast strains are isogenic with S288C. Epitope tagging and gene deletions were performed by PCR-based methods (Knop *et al.*, 1999; Janke *et al.*, 2004). *GFP-TUB1*, *mCherry-TUB1* (monomeric-Cherry), Gal1-*CDC5*, Met3-*3HA-CDC20*, and Met25-*KIN4* strains were constructed using integration plasmids (Caydasi *et al.*, 2010). Basic yeast methods and growth media were as described previously (Sherman, 1991).

Yeast strains were grown in yeast/peptone/dextrose medium with additional 0.1 mg/l adenine (YPDA) at 30°C unless otherwise specified. Plasmid-bearing strains were grown in synthetic complete (SC)

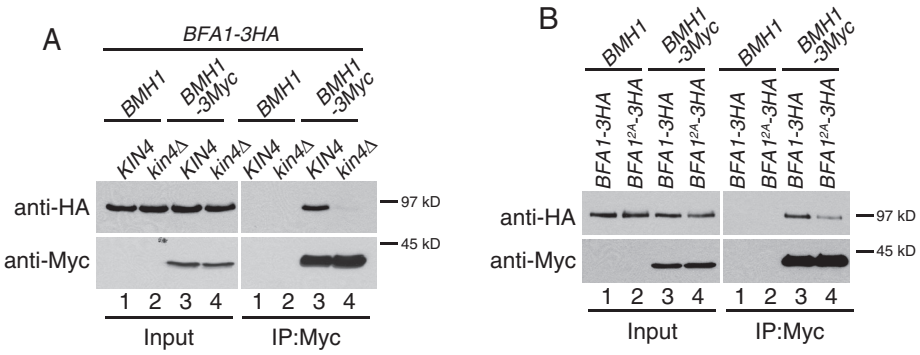

FIGURE 6: Bmh1 binds Bfa1 in a Kin4-dependent manner in vivo. (A) Coimmunoprecipitation of Bfa1-3HA with Bmh1-3Myc using *KIN4* and *kin4Δ* cells arrested in metaphase after nocodazole treatment. (B) Coimmunoprecipitation of Bfa1-3HA and Bfa1^{2A}-3HA with Bmh1-3Myc using yeast cells arrested in metaphase after nocodazole treatment.

medium/agar plates lacking the selective amino acid. For live-cell imaging, yeast cultures were grown in filter-sterilized SC media. Synthetic α-factor (Sigma-Aldrich, St. Louis, MO) at 10 μg/ml was added to the log-phase cultures for synchronization of the cells in G1. Release from G1 block was performed by washing and resuspending the cells in α-factor–free media. For nocodazole arrest, 15 μg/ml nocodazole (Sigma-Aldrich) was added to filter-sterilized YPDA medium. Induction of Gal1 promoter was done by addition of 2% galactose to the yeast cultures growing in 3% raffinose-containing medium, whereas suppression was done by addition of 2% glucose. Induction of Met3 and Met25 promoters was done in SC media or agar plates lacking methionine and cysteine (SC-Met-Cys). Met3 promoter was shut down by addition of 2 mM methionine and 2 mM cysteine to the log-phase cultures.

Induction of spindle misalignment

KAR9-deleted strains were kept complemented with *KAR9* on a *URA3*-based low–copy number plasmid. Experiments with *kar9Δ* cells were done after plasmid loss on 5-fluoroorotic acid–containing plates. To induce spindle misalignment, log-phase *kar9Δ* cultures grown at 23°C were shifted to 30°C for 1 or 3–4 h before time-lapse/FRAP or endpoint analysis, respectively. *DYN1*-deleted strains were grown at 30°C and shifted to 18°C for ~15 h to induce spindle misalignment before sample collection.

Fluorescence microscopy procedures

Time-lapse and FRAP experiments were performed as described in Caydasi and Pereira (2009) and Caydasi *et al.* (2010). Briefly, cells were attached on glass-bottom dishes (MatTek Corp., Ashland, MA) using 6% concanavalin A type IV (Sigma-Aldrich) and imaged at 30°C using a DeltaVision RT wide-field fluorescence imaging system (Applied Precision, Issaquah, WA) equipped with a quantifiable laser module, an Olympus IX71 microscope with plan-Apo 100×/numerical aperture (NA) 1.4 oil immersion objective (Olympus, Tokyo, Japan), a Photometrics CoolSnap HQ camera (Roper Scientific, Tucson, AZ), and SoftWoRx software (Applied Precision). Quad-mCh polychroic turret was in place. For time-lapse movies, 12 *z*-stacks of 0.3-μm optical section spacing were taken at each time point. Movies were taken for 60–90 min with 1-min time interval. For FRAP of Bfa1-GFP, four *z*-stacks of 0.3-μm thickness were acquired at each time point. Three and 160 images were acquired before and after photobleaching, respectively, with 2-s time interval. The *z*-stacks were sum-projected using SoftWoRx software before image analysis. Image analysis was done using ImageJ (National Institutes of Health, Bethesda, MD) by measuring the mean fluorescence intensity of the signal at a fixed-size area (0.595 μm^2). Mean fluorescence intensities were corrected for background and acquisition bleaching and normalized for prebleach intensity and photobleaching as described in Caydasi and Pereira (2009). FRAP recovery curves were fit to a single-exponential curve using IgorPro 6.02 software (Wavemetrics, Lake Oswego, OR).

Still images were acquired using a Zeiss Axiophot microscope equipped with a 100×/NA 1.45 Plan-Fluor oil immersion

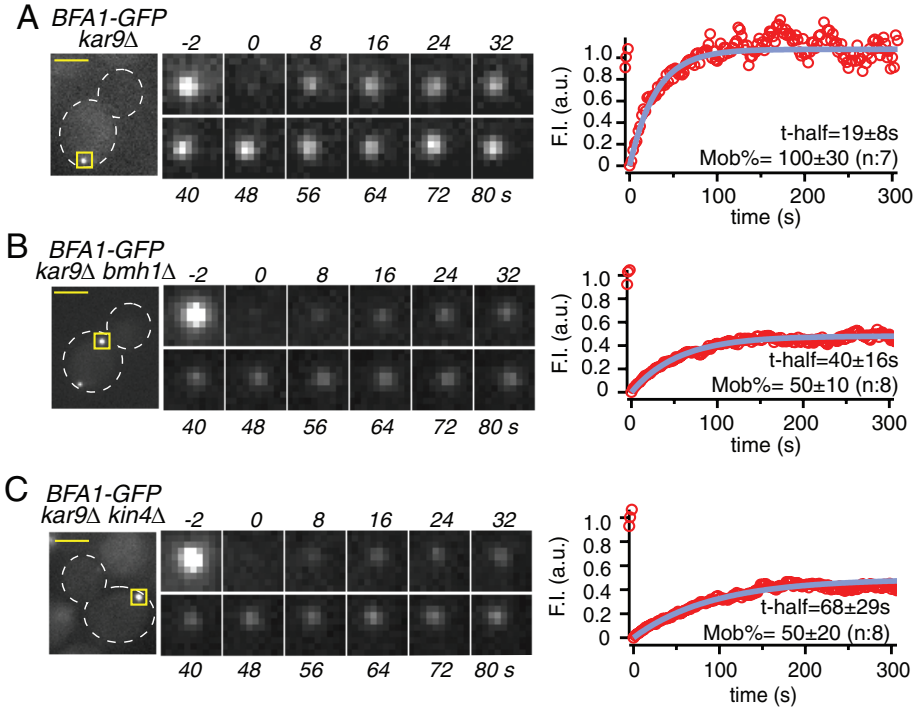

FIGURE 7: Bmh1 is crucial for dissociation of Bfa1 from the SPBs during spindle misalignment. (A–C) FRAP analysis of Bfa1-GFP in *kar9Δ* cells with misaligned spindles in the presence (A) or absence of *BMH1* (B) or *KIN4* (C). Still images of a representative FRAP experiment. Cell boundaries and the photobleached SPB are marked with dashed lines and solid squares, respectively. Time-lapse series show threefold-enlarged photobleached regions at the indicated time points. Time zero is the first image taken after photobleaching. The graphs show the average fluorescence recovery curves for the corresponding strains. Blue line depicts the best-fit single-exponential curve for each data set. $t_{1/2}$, half recovery time; Mob%, mobile fraction in percentage. Data represent the mean ± SD. *n*, number of samples. Fluorescence intensity (FI) is in arbitrary units (a.u.). Scale bars, 3 μm.

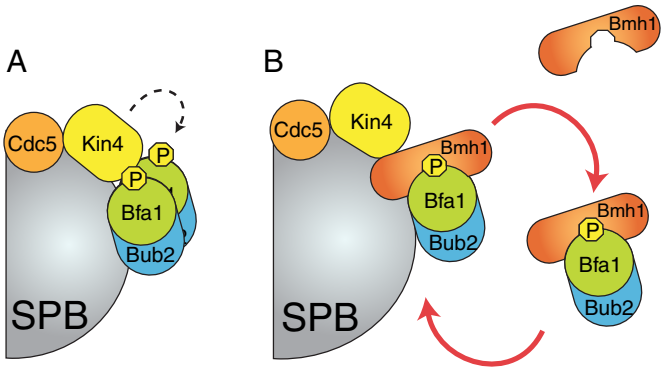

FIGURE 8: Working model for the regulation of Bfa1-Bub2 SPB association under SPOC- activating conditions. Bfa1 and Bub2 localizes to the SPBs as a complex (Pereira *et al.*, 2000; Caydasi and Pereira, 2009). Upon spindle misalignment, Kin4 phosphorylates Bfa1 (A). This phosphorylation creates a docking site for Bmh1, which in turn induces dynamic association of Bfa1 with the SPBs (B).

objective (Carl Zeiss, Jena, Germany), Cascade 1K charge-coupled device camera (Photometrics, Tucson, AZ), and MetaMorph software (Universal Imaging, Chesterfield, PA). Twelve *z*-stacks of 0.3-µm optical section spacing were acquired for each image. For single-time-point fluorescence images, yeast cultures concentrated by gentle centrifugation (2 min at 3200 rpm) were visualized without cell fixation (Kin4-GFP and Bfa1-GFP) or after cell fixation with 4% paraformaldehyde (GFP-tubulin). For budding index counting, cells were fixed with 70% ethanol and resuspended in phosphate-buffered saline (PBS) containing 1 µg/ml 4′,6-diamino-2-phenylindole (Sigma-Aldrich). The size of the buds and the distribution of DNA-stained regions were counted for 100–150 cells/time point.

Images were processed in ImageJ, Photoshop CS3 (Adobe, San Jose, CA), and Illustrator CS3 (Adobe). No manipulations were performed other than brightness, contrast, and color balance adjustments.

Protein methods

Yeast protein extracts and Western blotting were performed as described (Janke *et al.*, 2004). Antibodies were rabbit anti-GFP, goat anti-GST (GE Healthcare, Waukesha, WI), mouse anti-hemagglutinin (HA), rabbit anti-Clb2, guinea pig anti-Sic1, rabbit anti–P-S150 (Maekawa *et al.*, 2007), rabbit antixP-S180 (Maekawa *et al.*, 2007), mouse anti-Myc (9E10; Roche, Basel, Switzerland), mouse anti-tubulin (TAT1; Sigma-Aldrich), and mouse anti-MBP (New England BioLabs, Ipswich, MA). The anti-Kin4 antibody was raised in rabbits against the bacterially purified 6His-Kin4$^{361\text{-}750}$. Secondary antibodies were goat anti-mouse, goat anti-rabbit, rabbit anti-goat, and goat anti-guinea pig immunoglobulin G's coupled to horseradish peroxidase (Jackson ImmunoResearch Laboratories, West Grove, PA).

Recombinant protein purifications

MBP-Bfa1, MBP-Bfa1^{S150A}, MBP-Bfa1^{S180A}, and MBP-Bfa1^{2A} were purified from *Escherichia coli* as described previously (Maekawa *et al.*, 2007; Geymonat *et al.*, 2009). GST-Bmh1 was induced in *E. coli* BL21 (DE3) at 23°C and purified according to the manufacturer's instructions.

Immunoprecipitation experiments

From 100 to 150 ml (2×10^7 cells/ml) of culture pellet was lysed using acid-washed glass beads in a FastPrep FP120 Cell Disturber (MP Biomedicals, Irvine, CA). Lysis buffer was Tris-HCl buffer (50 mM, pH 7.4) with 10% glycerol containing 350 µg/ml benzamidine, 100 mM β-glycerophosphate, 50 mM NaF, 5 mM $NaVO_3$ and complete EDTA-free protease inhibitor cocktail (Roche). The amount of NaCl in the lysis buffer was 100, 150, and 400 mM for Bfa1, Bmh1, and Kin4 immunoprecipitations, respectively. Lysates were incubated with detergent for 10 min, and total extracts were cleared by centrifugation at 10,621 × *g* for 10 min. Detergents were 0.5% Triton X-100, 0.2% Triton X-100, and 1% nonyphenylpolyethylane glycol (NP-40) for Bfa1, Bmh1, and Kin4 immunoprecipitations, respectively. Bfa1-9Myc and Bmh1-3Myc, Kin4-6HA, or GST-Kin4 were immunoprecipitated using anti-Myc coupled protein A–Sepharose beads (GE Healthcare), anti-HA coupled protein A–Sepharose beads (GE Healthcare), or glutathione–Sepharose beads (GE Healthcare), respectively.

In vitro binding assay

MBP-Bfa1 purified from *E. coli* was incubated at 30°C for 45 min with yeast-enriched GST-Kin4 (wild type) and GST-Kin4^{T209A} (kinase-dead mutant; D'Aquino *et al.*, 2005) bound Sepharose beads (GE Healthcare) in kinase buffer (20 mM 4-(2-hydroxyethyl)-1-piperazineethanesulfonic acid [HEPES], pH 7.4, 0.5 mM EDTA, 0.5 mM dithiothreitol [DTT], 20 mM $MgCl_2$, 10 mM β-glycerophosphate, 0.625 mM ATP). The supernatant of the kinase reaction was then incubated with GST-Bmh1 bound to glutathione–Sepharose beads (GE Healthcare) at 4°C for 30 min. GST-Bmh1–bound beads were washed with PBS containing 0.75% NP-40, and samples were boiled with HU-DTT (200 mM Tris-HCl, pH 6.8, 8 M urea, 5% SDS, 0.1 mM EDTA, 0.005% bromophenol blue, and 15 mg/ml DTT) buffer before SDS–PAGE.

Radioactive kinase reactions

For radioactive kinase assays of immunoprecipitated Kin4-6HA, reaction buffer contained 20 mM HEPES, pH 7.4, 0.5 mM EDTA, 0.5 mM DTT, 20 mM $MgCl_2$, 10 mM β-glycerophosphate, 0.04 mM ATP, 3 µCi of [γ-^{32}P]ATP (0.03 nM), and MBP-Bfa1 purified from *E. coli*. Reactions were carried out at 30°C for 20 min. Samples were boiled in sample buffer (62.5 mM Tris-HCl, pH 6.8, 2% SDS, 5% β-mercaptoethanol, 10% glycerol, 0.02% bromophenol blue) before SDS–PAGE.

Quantification of relative band intensities from immunoblots and radiographs

For quantitative analysis of protein bands, chemiluminescence from immunoblots was detected in a LAS-3000 imager (FujiFilm, Tokyo, Japan). Incorporation of ^{32}P in MBP-Bfa1 was detected using a FujiFilm BAS 1800-II imaging system. Relative protein band intensities were determined using ImageJ software and were corrected against the gel background signal. Relative levels of Kin4 phosphorylated Bfa1 (Figure 2C) were calculated by dividing the intensity of anti–P-S180 by anti-Myc–detected protein bands. All three samples (Bfa1-9Myc immunoprecipitated from Gal1-*KIN4*, *kin4*Δ, and Gal1-*KIN4 bmh1*Δ) were always present on the same membrane. Specific Kin4 kinase activity (Supplemental Figure S3C) was calculated by dividing the amount of ^{32}P incorporated in MBP-Bfa1 by the relative amounts of immunoprecipitated Kin4-6HA.

ACKNOWLEDGMENTS

We acknowledge Elmar Schiebel and Ingrid Grummt for sharing reagents and equipment, Iain Hagan and Elmar Schiebel for critically reading the manuscript, and workers from G.P.'s lab for comments. This work was supported by Deutsche Forschungsgemeinschaft

grant PE1883/1 to G.P. A.K.C. and Y.M. were funded by Deutsche Forschungsgemeinschaft Grant PE1883/1.

REFERENCES

Bardin AJ, Amon A (2001). Men and sin: what's the difference? Nat Rev Mol Cell Biol 2, 815–826.

Bardin AJ, Visintin R, Amon A (2000). A mechanism for coupling exit from mitosis to partitioning of the nucleus. Cell 102, 21–31.

Bloecher A, Venturi GM, Tatchell K (2000). Anaphase spindle position is monitored by the BUB2 checkpoint. Nat Cell Biol 2, 556–558.

Bolton DL, Barnitz RA, Sakai K, Lenardo MJ (2008). 14-3-3 theta binding to cell cycle regulatory factors is enhanced by HIV-1 Vpr. Biol Direct 3, 17.

Caydasi AK, Kurtulmus B, Orrico MI, Hofmann A, Ibrahim B, Pereira G (2010). Elm1 kinase activates the spindle position checkpoint kinase Kin4. J Cell Biol 190, 975–989.

Caydasi AK, Lohel M, Grunert G, Dittrich P, Pereira G, Ibrahim B (2012). A dynamical model of the spindle position checkpoint. Mol Syst Biol 8, 582.

Caydasi AK, Pereira G (2009). Spindle alignment regulates the dynamic association of checkpoint proteins with yeast spindle pole bodies. Dev Cell 16, 146–156.

Caydasi AK, Pereira G (2012). SPOC alert—when chromosomes get the wrong direction. Exp Cell Res 318, 1421–1427.

Cottingham FR, Hoyt MA (1997). Mitotic spindle positioning in *Saccharomyces cerevisiae* is accomplished by antagonistically acting microtubule motor proteins. J Cell Biol 138, 1041–1053.

D'Aquino KE, Monje-Casas F, Paulson J, Reiser V, Charles GM, Lai L, Shokat KM, Amon A (2005). The protein kinase Kin4 inhibits exit from mitosis in response to spindle position defects. Mol Cell 19, 223–234.

Foley EA, Kapoor TM (2013). Microtubule attachment and spindle assembly checkpoint signalling at the kinetochore. Nat Rev Mol Cell Biol 14, 25–37.

Fraschini R, Formenti E, Lucchini G, Piatti S (1999). Budding yeast Bub2 is localized at spindle pole bodies and activates the mitotic checkpoint via a different pathway from Mad2. J Cell Biol 145, 979–991.

Fu H, Subramanian RR, Masters SC (2000). 14-3-3 proteins: structure, function, and regulation. Annu Rev Pharmacol Toxicol 40, 617–647.

Gardino AK, Yaffe MB (2011). 14-3-3 proteins as signaling integration points for cell cycle control and apoptosis. Semin Cell Dev Biol 22, 688–695.

Geymonat M, Spanos A, de Bettignies G, Sedgwick SG (2009). Lte1 contributes to Bfa1 localization rather than stimulating nucleotide exchange by Tem1. J Cell Biol 187, 497–511.

Geymonat M, Spanos A, Smith SJ, Wheatley E, Rittinger K, Johnston LH, Sedgwick SG (2002). Control of mitotic exit in budding yeast. In vitro regulation of Tem1 GTPase by Bub2 and Bfa1. J Biol Chem 277, 28439–28445.

Geymonat M, Spanos A, Walker PA, Johnston LH, Sedgwick SG (2003). In vitro regulation of budding yeast Bfa1/Bub2 GAP activity by Cdc5. J Biol Chem 278, 14591–14594.

Grandin N, Charbonneau M (2008). Budding yeast 14-3-3 proteins contribute to the robustness of the DNA damage and spindle checkpoints. Cell Cycle 7, 2749–2761.

Hoyt MA, Totis L, Roberts BT (1991). *S. cerevisiae* genes required for cell cycle arrest in response to loss of microtubule function. Cell 66, 507–517.

Hu F, Wang Y, Liu D, Li Y, Qin J, Elledge SJ (2001). Regulation of the Bub2/Bfa1 GAP complex by Cdc5 and cell cycle checkpoints. Cell 107, 655–665.

Janke C *et al.* (2004). A versatile toolbox for PCR-based tagging of yeast genes: new fluorescent proteins, more markers and promoter substitution cassettes. Yeast 21, 947–962.

Johnson C, Crowther S, Stafford MJ, Campbell DG, Toth R, MacKintosh C (2010). Bioinformatic and experimental survey of 14-3-3-binding sites. Biochem J 427, 69–78.

Knop M, Siegers K, Pereira G, Zachariae W, Winsor B, Nasmyth K, Schiebel E (1999). Epitope tagging of yeast genes using a PCR-based strategy: more tags and improved practical routines. Yeast 15, 963–972.

Kostelecky B, Saurin AT, Purkiss A, Parker PJ, McDonald NQ (2009). Recognition of an intra-chain tandem 14-3-3 binding site within PKCepsilon. EMBO Rep 10, 983–989.

Li R, Murray AW (1991). Feedback control of mitosis in budding yeast. Cell 66, 519–531.

Maekawa H, Priest C, Lechner J, Pereira G, Schiebel E (2007). The yeast centrosome translates the positional information of the anaphase spindle into a cell cycle signal. J Cell Biol 179, 423–436.

McNally FJ (2013). Mechanisms of spindle positioning. J Cell Biol 200, 131–140.

Miller RK, Rose MD (1998). Kar9p is a novel cortical protein required for cytoplasmic microtubule orientation in yeast. J Cell Biol 140, 377–390.

Molla-Herman A, Boularan C, Ghossoub R, Scott MG, Burtey A, Zarka M, Saunier S, Concordet JP, Marullo S, Benmerah A (2008). Targeting of beta-arrestin2 to the centrosome and primary cilium: role in cell proliferation control. PLoS One 3, e3728.

Monje-Casas F, Amon A (2009). Cell polarity determinants establish asymmetry in MEN signaling. Dev Cell 16, 132–145.

Obsilova V, Nedbalkova E, Silhan J, Boura E, Herman P, Vecer J, Sulc M, Teisinger J, Dyda F, Obsil T (2008). The 14-3-3 protein affects the conformation of the regulatory domain of human tyrosine hydroxylase. Biochemistry 47, 1768–1777.

Pereira G, Hofken T, Grindlay J, Manson C, Schiebel E (2000). The Bub2p spindle checkpoint links nuclear migration with mitotic exit. Mol Cell 6, 1–10.

Pereira G, Schiebel E (2005). Kin4 kinase delays mitotic exit in response to spindle alignment defects. Mol Cell 19, 209–221.

Pereira G, Tanaka TU, Nasmyth K, Schiebel E (2001). Modes of spindle pole body inheritance and segregation of the Bfa1p-Bub2p checkpoint protein complex. EMBO J 20, 6359–6370.

Pietromonaco SF, Seluja GA, Aitken A, Elias L (1996). Association of 14-3-3 proteins with centrosomes. Blood Cells Mol Dis 22, 225–237.

Shen YH, Godlewski J, Bronisz A, Zhu J, Comb MJ, Avruch J, Tzivion G (2003). Significance of 14-3-3 self-dimerization for phosphorylation-dependent target binding. Mol Biol Cell 14, 4721–4733.

Sherman F (1991). Getting started with yeast. Methods Enzymol 194, 3–21.

Trembley MA, Berrus HL, Whicher JR, Humphrey-Dixon EL (2014). The yeast 14-3-3 proteins Bmh1 and Bmh2 differentially regulate rapamycin-mediated transcription. Biosci Rep 34, 119–126.

Usui T, Petrini JH (2007). The *Saccharomyces cerevisiae* 14-3-3 proteins Bmh1 and Bmh2 directly influence the DNA damage-dependent functions of Rad53. Proc Natl Acad Sci USA 104, 2797–2802.

Valerio-Santiago M, Monje-Casas F (2011). Tem1 localization to the spindle pole bodies is essential for mitotic exit and impairs spindle checkpoint function. J Cell Biol 192, 599–614.

van Heusden GP, Steensma HY (2006). Yeast 14-3-3 proteins. Yeast 23, 159–171.

Veisova D, Rezabkova L, Stepanek M, Novotna P, Herman P, Vecer J, Obsil T, Obsilova V (2010). The C-terminal segment of yeast BMH proteins exhibits different structure compared to other 14-3-3 protein isoforms. Biochemistry 49, 3853–3861.

Wang C, Skinner C, Easlon E, Lin SJ (2009). Deleting the 14-3-3 protein Bmh1 extends life span in *Saccharomyces cerevisiae* by increasing stress response. Genetics 183, 1373–1384.

Yaffe MB (2002). How do 14-3-3 proteins work?—gatekeeper phosphorylation and the molecular anvil hypothesis. FEBS Lett 513, 53–57.

Yaffe MB, Rittinger K, Volinia S, Caron PR, Aitken A, Leffers H, Gamblin SJ, Smerdon SJ, Cantley LC (1997). The structural basis for 14-3-3: phosphopeptide binding specificity. Cell 91, 961–971.

Yeh E, Skibbens RV, Cheng JW, Salmon ED, Bloom K (1995). Spindle dynamics and cell cycle regulation of dynein in the budding yeast, *Saccharomyces cerevisiae*. J Cell Biol 130, 687–700.